COMPARISON BETWEEN SURVEY RADIOGRAPHY, B-MODE ULTRASONOGRAPHY, CONTRAST-ENHANCED ULTRASONOGRAPHY AND CONTRAST-ENHANCED MULTI-DETECTOR COMPUTED TOMOGRAPHY FINDINGS IN DOGS WITH ACUTE ABDOMINAL SIGNS

MIRIAM M. SHANAMAN, TOBIAS SCHWARZ, ARNON GAL, ROBERT T. O'BRIEN

Contrast-enhanced multi-detector computed tomography (CE-MDCT) is used routinely in evaluating human patients with acute abdominal symptoms. Contrast-enhanced ultrasound (CEUS) continues to be in its infancy as it relates to evaluation of the acute abdomen. The purpose of this study was to compare survey radiography, B-mode ultrasound, CEUS, and CE-MDCT findings in canine patients presenting with acute abdominal signs; with a focus on the ability to differentiate surgical from non-surgical conditions. Nineteen dogs were prospectively enrolled. Inclusion required a clinical diagnosis of acute abdominal signs and confirmed surgical or non-surgical causes for the clinical signs. Agreement for the majority of recorded imaging features was at least moderate. There was poor agreement in the identification of pneumoperitoneum and in the comparison of pancreatic lesion dimensions for B-mode vs. CEUS. The CT feature of fat stranding was detected in cases including, but not limited to, gastric neoplasia with perforation, pancreatitis, and small intestinal foreign body. Ultrasound underestimated the size and number of specific lesions when compared with CE-MDCT. Contrast-enhanced ultrasound was successful in detecting bowel and pancreatic perfusion deficits that CE-MDCT failed to identify. Accuracy for differentiation of surgical vs. non-surgical conditions was high for all modalities; 100%, 94%, and 94% for CE-MDCT, ultrasonography and survey radiography respectively. Findings indicated that CE-MDCT is an accurate screening test for differentiating surgical from non-surgical acute abdominal conditions in dogs. Focused CEUS following CE-MDCT or B-mode ultrasonography may be beneficial for identifying potentially significant hypoperfused lesions. © 2013 *Veterinary Radiology & Ultrasound.*

Key words: acute abdomen, dog, CT, contrast.

Introduction

DIAGNOSTIC IMAGING PLAYS A pivotal role in the initial assessment of dogs with acute abdominal signs. The ability to obtain a rapid and accurate diagnosis is paramount in guiding appropriate medical and or surgical intervention. Survey radiography and abdominal ultrasonography are the current standard imaging modalities for evaluation of dogs with acute abdominal signs. Ultrasonographic characteristics of canine pancreatitis[1–7] and neoplastic and non-neoplastic diseases of the gastrointestinal (GI) tract[8–16] are well-described in the veterinary literature, as these conditions compose a large majority of canine acute abdominal diseases. The benefits of ultrasound (US) in identification of GI tract perforation and characterization of pneumoperitoneum have also been described.[17,18] Multiple veterinary studies have shown that abdominal ultrasonography improves detection of GI foreign bodies and has improved accuracy for the diagnosis of mechanical ileus when survey radiographic results are equivocal.[19,20] Furthermore, while routine ultrasonography is inferior in the detection of pneumoperitoneum when compared with radiography and computed tomography (CT) in people, the improved detection of small volumes of peritoneal free fluid is considered beneficial.[21,22] Abdominal ultrasound, however, is characterized by additional unique limitations including inter-operator variability, possible patient discomfort, duration of study acquisition, limited field of view, and possible interference/lack of visibility of organs of interest due to overlying bowel or peritoneal free gas.

From the Department of Veterinary Clinical Medicine, University of Illinois at Urbana-Champaign, Urbana, IL 61802 (Shanaman, O'Brien); Division of Clinical Sciences, Royal (Dick) School of Veterinary Studies, University of Edinburgh, Roslin, Midlothian, Scotland, UK (Schwarz); and Department of Pathobiology, University of Illinois at Urbana-Champaign, Urbana, IL 61802 (Gal).

Source of Support: We thank the Dr. Allan L. and Mary L. Graham Endowment for financial support.

Previous Presentations/Abstracts: ACVR 2012, Las Vegas, NV, USA.

Address correspondence and reprint requests to Miriam M. Shanaman, at the above address. E-mail: miriamshanaman@gmail.com

Received February 5, 2013; accepted for publication May 18, 2013.
doi: 10.1111/vru.12079

With the development and increased availability of multidetector helical CT (MDCT), survey radiography has largely fallen out of favor in the human emergency room due to its relatively poor sensitivity and specificity. The survey radiographic detection of pneumoperitoneum remains potentially advantageous, however, with reported sensitivities as high as 98% in human patients.[23]

Computed tomography evaluation of the canine abdomen has been described in a small number of studies that have included characterization of conditions of the upper and lower urinary tract,[24–30] spleen,[31–33] hepatic/portal venous abnormalities,[34–46] pancreas,[7,47,48] mesenteric/intrapelvic neoplasia,[49,50] adrenal gland,[51–53] and gastrointestinal tract.[54,55] A recent study described a sedated contrast-enhanced CT protocol in clinical canine patients.[56] In a separate study by the same group, this same protocol successfully detected a greater number of lesions than routine abdominal ultrasonography in patients weighing greater than 25 kg.[57] Our group has recently demonstrated that dual-phase CE-MDCT is feasible and safe in both awake and minimally sedated canine patients with acute abdominal signs.[58]

The primary goal of the current study was to assess agreement among survey radiography, B-mode ultrasonography, contrast-enhanced US (CEUS), and CE-MDCT for detecting specific intra-abdominal lesions and for differentiating surgical versus non-surgical acute abdominal conditions. We hypothesized that, for the majority of imaging findings, CT and ultrasonography would have at least good agreement. A second goal of our study was to describe accuracy for the differentiation of surgical versus non-surgical conditions across modalities. We hypothesized that CE-MDCT would have the highest accuracy for differentiating surgical from non-surgical conditions when a diagnosis could be made with imaging findings alone. We hypothesized that CE-MDCT would show a trend toward identifying both larger and a greater number of non-enhancing lesions when compared with CEUS. A third goal of our study was to introduce a specific CT lesion termed fat stranding. This lesion is defined as an abnormal increased attenuation in fat[59] and has been described in human studies as an imaging feature associated with severe inflammatory and ischemic conditions of the pancreas and bowel.[60–64]

Materials and Methods

All protocols were approved by the Institutional Animal Care and Use Committee of the University of Illinois. Client-owned dogs that were presented to the University of Illinois Veterinary Teaching Hospital between December 2010 and January 2012 for acute abdominal signs were prospectively enrolled following owner consent. Study enrollment required the cytologic, survey radiographic, and/or sonographic detection of a condition requiring immediate surgical intervention (visceral abscess, traumatic diaphragmatic hernia, spontaneous pneumoperitoneum, or small intestinal mechanical obstruction) or alternatively sonographic changes consistent with acute pancreatitis[1–7,65] or GI neoplasia.[9,10,12,14,15] In the case of acute pancreatitis, results of pancreatic fine-needle aspiration with cytology and cPLI were also required. Self-limiting cases of gastroenteritis or functional ileus were excluded because a sensitive and specific antemortem test for use as a reference standard was not available.

Clinical data recorded included breed, age (years), gender (male vs.female), spay/neuter status, duration, and type of clinical signs (days), select physical examination findings (rectal temperature, heart rate, blood pressure, hydration status, presence, and severity of abdominal pain), and select laboratory findings when available (serum lactate, serum creatinine, and urine-specific gravity).

All patients enrolled were required to undergo routine abdominal radiography, B-mode and CEUS, and CE-MDCT. All radiographic images were reviewed by two board-certified radiologists (TS, RTO) and the primary author (MMS) on dedicated DICOM workstations with calibrated monitors. Radiographic studies were randomized and the reviewers were unaware of patient signalment, clinical signs, and final diagnosis at the time of interpretation. As an additional reviewer bias control, eight additional digitally acquired three-view abdominal radiographic studies of normal or non-acute abdominal conditions were incorporated randomly into the study population for interpretation but not statistical analysis. A consensus was achieved for all variables evaluated. Categorical variables recorded included the following: presence/absence of specific lesions (pneumoperitoneum, small intestinal plication, visible small intestinal foreign material); presence of small bowel distension as previously described[66] (duodenum only, portion of jejunum, duodenum and portion of jejunum, all small bowel); and surgical vs. medical condition (based on imaging findings alone). Peritoneal serosal detail was considered as an ordinal variable (normal detail, focal loss of detail, multifocal loss of detail, and generalized loss of detail).

All patients underwent routine abdominal B-mode ultrasonography with a dedicated ultrasonography machine (MyLab70 XVG, Esaote, Indianapolis, IN). A microconvex curvilinear array transducer (3–9 MHz) and/or linear array transducer (4–13 MHz) were utilized. Probe selection and frequency, depth of field, overall gain, time-gain compensation, and focal zone were adjusted at the discretion of the sonographer to optimize image quality. The dedicated sonographer was either the primary resident or board-certified imaging faculty member responsible for the ultrasonography service at the time of patient admission. Categorical variables were recorded as

presence/absence of specific lesions (pneumoperitoneum, hyperechoic mesentery, small intestinal plication, visible small intestinal foreign body); visible zone of transition if bowel plication/distension (not identified, proximal jejunum, mid jejunum, distal jejunum); location of small intestinal dilation if present (duodenum only, portion of jejunum, duodenum and portion of jejunum, all small bowel); and surgical vs. medical condition (on the basis of imaging findings alone). Volume of peritoneal free fluid (none, focal, multifocal, generalized) was considered as an ordinal variable.

Routine B-mode ultrasonography was immediately followed by CEUS of any lesion(s) interpreted by the sonographer to have questionable perfusion deficits using the same machine fitted with a variable band array linear transducer (3–11 MHz) utilizing specific contrast software (CnTI™, Esaote, Indianapolis, IN). Lesions were considered to have questionable perfusion deficits on B-mode ultrasonography if a relatively hypoechoic or cavitary parenchymal lesion was identified, if there was a possibility of visceral entrapment, or at the site of a small intestinal foreign body or significant gastric/intestinal wall thickening. Power and mechanical indices used were 5% and 0.03, respectively. Overall gain, depth of field and focal zone were adjusted at the discretion of the sonographer to maximize image quality. The region of interest for CEUS was initially isolated in gray-scale images. Split-screen technology was used in order to simultaneously visualize gray-scale and contrast-enhanced images respectively. One to two rapid bolus injections of microbubble contrast agent (Definity, Lantheus Medical Imaging, North Billerica, MA) were administered for each lesion in question. For patients weighing <20 kg, 0.1 ml of contrast was administered each time as a rapid intravenous bolus followed by a 2–3 ml 0.9% NaCl flush. For patients weighing >20 kg, 0.2 ml of contrast medium was administered each time as a rapid intravenous bolus, likewise followed by a 2–3 ml 0.9% NaCl flush. An initial clip was obtained in all cases until subjective peak parenchymal enhancement (initiation of wash-out phase). Additional clips and/or still images were collected as deemed necessary by the attending sonographer to document a persistent lack or relative reduction in contrast enhancement of a specific lesion compared to surrounding tissue when identified. Routine B-mode and CEUS images were evaluated prospectively at the time the scan was performed and again retrospectively by a single reviewer (MMS) for recording of the following characteristics: presence of persistently non-enhancing or relatively hypoperfused pancreatic, gastric or small intestinal wall lesions (relative to contrast enhancing adjacent tissue); total number of hypoperfused lesions (liver, spleen); and estimated size of the largest hypoperfused lesion on pre vs.postcontrast images (pancreas, liver). With the exception of patients with acute pancreatitis, all lesions considered hypoperfused following CEUS evaluation were confirmed histologically or cytologically.

All patients underwent dual-phase contrast-enhanced abdominal CT using a 16-slice helical CT scanner (GE Lightspeed 16 Slice CT Milwaukee, WI, USA) using the following parameters: kV of 120, mA of 100–325, slice width (SW) of 2.5 mm (with 1.25 mm overlap), scan field of view of 25–50 cm, 512 × 512 matrix, collimator pitch of 0.9–1.3:1 and rotation time of 0.5–0.8 s. Subsequent multiplanar reformatting was performed on the raw data in all patients to obtain reconstructed images in the dorsal and sagittal planes with a 0.625 mm SW. A dose of 2 ml/kg (600 mg I/kg) non-ionic iodinated contrast (Omnipaque 300™ Iohexol injection, GE Healthcare, Princeton, NJ) was administered intravenously in all patients with a maximum total dose set at 60 ml. The contrast agent was administered as a hand injected fast bolus in patients weighing ≤20 lbs. In patients ≥20 lbs, the contrast agent was administered via power injector (Medrad Vistron CT Injection System®, Indianola, PA) at a rate of 3 ml/s followed by a 10 ml 0.9% saline flush. Every attempt was made to scan patients awake, and intravenous sedation was used when these attempts were unsuccessful. All scans were considered diagnostic based on previously established criteria and delayed scans (when available) were evaluated to rule out immediate contrast-related acute renal injury.[58]

The primary transverse CT images (pre-contrast, arterial, and portal venous phases) in addition to dorsal and sagittal plane reformatted images were reviewed in a randomized blinded fashion by two board-certified radiologists (TS, RTO) and the primary author (MMS) on dedicated DICOM workstations with calibrated monitors. To prevent reviewer bias, eight additional CE-MDCT studies requiring a minimum of a dual phase protocol were incorporated randomly into the study population for interpretation but not statistical analysis. The reviewers were unaware of patient signalment, clinical history, or final diagnosis at the time of interpretation. Window width and level could be adjusted at the discretion of the reviewer. Consensus was achieved for all variables evaluated. Categorical variables evaluated were recorded as follows: presence or absence of specific lesions (pneumoperitoneum, fat stranding, small intestinal plication, visible small intestinal foreign material); presence of small bowel distension (duodenum only, portion of jejunum, duodenum and portion of jejunum, all small bowel); visible zone of transition if bowel plication/distension (duodenal, proximal jejunal, mid jejunal, distal jejunal); and surgical vs. medical condition (on the basis of imaging findings alone). Presence of peritoneal free fluid (none, focal, multifocal, generalized) was considered as an ordinal variable. On post-contrast venous images, the presence of persistently non-enhancing pancreatic, gastric or small intestinal wall lesions; total number of non-enhancing lesions (liver, spleen); and estimated size of

the largest non-enhancing lesion if present (liver, pancreas) were also recorded.

Exploratory laparotomy or necropsy with histopathology was considered the reference standard for diagnosis of surgical underlying conditions (small intestinal mechanical obstruction, gastrointestinal perforation, traumatic diaphragmatic hernia or visceral abscess). Surgically excised and gross pathological lesions were evaluated histologically by a single pathologist (AG). Sample sections were selected following CT evaluation in an attempt to provide a precise histologic correlation.

Non-surgical conditions were confirmed at necropsy for cases that were humanely euthanized prior to discharge. For cases that survived to discharge, overall survival time (days) was recorded under the assumption that prolonged survival (greater than 30 days) suggested that the underlying condition in a given patient did not require immediate surgical intervention. In patients with sonographic evidence of acute pancreatitis, results of cPLI and US-guided fine-needle aspiration of the pancreas were also required for study inclusion.

All statistical tests were selected and performed by the primary author (MMS). Commercial software (SPSS IBM Company, Chicago, IL; MedCalc Version 12.3.0, Mariakerke, Belgium) was used for statistical analysis and a P-value < 0.05 was considered statistically significant. Continuous variables (age, duration of clinical signs, rectal temperature, heart rate, blood pressure, serum lactate, serum creatinine, urine specific gravity) were assessed for normality using a Shapiro–Wilk test.[67] For continuous data that met the assumption of normality, a Levene's test was performed to assess for homogeneity of variance.[68] For data that met the assumption of normality, mean, min–max, and standard deviation (SD) were recorded. For non-normally distributed continuous data, median and 25th–75th percentiles were reported.

Agreement between modalities for categorical and ordinal variables was assessed with a Cohen's Kappa coefficient and weighted Kappa, respectively, given that many of the imaging features listed are not characterized by a strict reference or gold standard. Interpretation of the Kappa coefficient was as follows: 0 = chance agreement, <0.2 = poor agreement, 0.21–0.40 = fair agreement, 0.41–0.60 = moderate agreement, 0.61–0.80 = good agreement, >0.8 = very good agreement, and 1.0 = perfect agreement.[69] To assess agreement between routine B-mode and CEUS findings related to the size of a hypoechoic or hypoperfused pancreatic lesion respectively, a Bland–Altman plot was generated.

Sensitivity (true positive rate), specificity (true negative rate), positive predictive value (PPV), negative predictive value (NPV), and accuracy for differentiation of surgical from non-surgical conditions was also assessed for each modality.

Results

Nineteen client-owned dogs were included in the study. Nine underwent awake diagnostic imaging while 10 received minimal sedation as previously described.[58] Breeds included one each of the following: Norwich Terrier, Tibetan Spaniel, Labrador Retriever, miniature Australian Shepherd, Bloodhound, Golden Retriever, Shetland Sheepdog, Scottish Terrier, Basenji, Shih Tzu, Yorkshire Terrier, American Pit Bull Terrier, Boxer, Pug, Pomeranian, Dachshund, and 3 mix-breed dogs. The mean age was 8.1 years (range 4–15.2, SD 3.2). Eight were female (all spayed) and 11 were male (four intact, seven neutered). Mean duration of clinical signs prior to presentation was 5 days (min–max 1–10, SD 2.9) with vomiting as the most commonly reported clinical sign (15/19, 79% of cases). Other reported clinical signs included anorexia/reduced appetite (12), lethargy (7), diarrhea (4), and respiratory distress (1). Mean rectal temperature at the time of presentation was 101.5°C (min–max 99.2–104, SD 1.1), mean heart rate was 123.4 bpm (min–max 88–160, SD 19.1), mean systolic blood pressure (measured in 18/19 cases) was 150.3 mmHg (min–max 70–200, SD 32.2), median serum lactate (measured in 17/19 cases) was 2.3 mmol/l (25th–75th percentile = 1.65–4), median serum creatinine (measured in 17/19 cases) was 0.8 mg/dl (25th–75th percentile = 0.7–0.95), and mean urine specific gravity (measured in 13/19 cases) was 1.030 (min–max 1.01–1.05, SD 0.02). Sixteen patients (84%) were considered clinically dehydrated; 10/16 (63%) mildly dehydrated, 3/16 (19%) moderately dehydrated, and 3/16 (19%) severely dehydrated. Fifteen patients (79%) were considered to have a painful abdomen on presentation. No immediate contrast-related adverse reactions were noted at the time of CE-MDCT or CEUS.

Thirteen of 19 (68%) cases had all imaging studies performed consecutively the same day (radiographs followed by CT/ultrasonography), 4/19 (21%) had all imaging studies performed within a 24 h period, 1/19 (5%) had all studies performed within a 48 h period, and 1/19 (5%) had ultrasonography and CT evaluation within 24 h, however, radiographs were obtained 6 days prior. A three-view abdominal series (right lateral, left lateral and ventrodorsal view) was obtained in 17/19 (89%) cases while a two-view series (right or left lateral and ventrodorsal view) was obtained in 2/19 (11%) cases. Eighteen of 19 radiographic series' were acquired digitally, while a single case had analog films obtained by the referring veterinarian that were later scanned into our PACS system. All cases underwent awake or minimally sedated CE-MDCT. In one case, an arterial post-contrast phase was not attempted and instead two sequential venous phases were obtained. This same patient was scanned awake in sternal recumbency within the VetMouseTrap™ (University of Illinois, Urbana, IL).

Eight patients (42%) were considered to have an underlying condition that was non-surgical (seven acute pancreatitis, one gastric B-cell lymphoma). In cases with ultrasonography findings consistent with acute pancreatitis (7/7, 100%),[1–7,65] a positive cPLI was identified in 5/7 (71%) cases and cytologic evidence of suppurative inflammation in 3/7 (43%) cases. The case of gastric B-cell lymphoma was diagnosed histologically following gross necropsy evaluation. Six of seven (86%) cases with acute pancreatitis survived to discharge with a mean survival of 427 days (range 103–634 days, SD 189). Five of these six cases remain alive to date. Prolonged duration of survival supports the assumption that these patients indeed suffered from a medical (rather than surgical) underlying condition.

Eleven patients (58%) were considered to have an underlying condition that would require surgical intervention. Ten of these cases had surgical and/or histologic confirmation of disease and all surgically excised lesions were submitted for histopathology: hepatic abscess secondary to anaplastic carcinoma, widespread metastatic hemangiosarcoma with splenic abscessation (Fig. 1), gastric B-cell lymphoma with perforation, linear foreign body (four cases; cloth, bandage material with sponge, multiple solid objects with fibrous connection, unknown material; Fig. 2), proximal jejunal obstructive corn cob foreign body (Fig. 3), combined gastric and jejunal obstructive cloth foreign bodies, and traumatic diaphragmatic hernia. One case of multifocal hepatic abscessation was diagnosed with cytology alone, as gross necropsy examination was not pursued. In the two cases of hepatic abscess formation, imaging alone was insufficient to make a definitive preoperative surgical diagnosis with any modality given the absence of parenchymal or free peritoneal gas. These cases required US-guided fine-needle aspiration and cytology of cavitary hepatic lesions for confirmation of surgical disease.

Statistical agreement among all modalities for the identification of specific categorical and ordinal imaging features is summarized in Table 1.

Survey radiography detected pneumoperitoneum in 2/19 (11%) cases. In 3/4 (75%) linear foreign body cases, small bowel plication was detected radiographically. Small intestinal foreign material was considered opaque/visible in 5/6 (83%) cases with confirmed small intestinal obstruction secondary to foreign material and small bowel distension detected radiographically in 4/6 (67%) cases. Six of 19 (32%) cases were considered to have loss of peritoneal serosal detail on survey radiographs. This was further characterized as generalized loss of serosal detail in 3/6 (50%) cases, focal loss of detail in 2/6 (33%) cases, and multifocal loss of detail in 1/6 (17%) cases. Survey radiography correctly identified 8/9 (89%) cases as surgical for which a conclusion could be made with imaging findings alone. The single false-negative radiographic diagnosis was a linear foreign body with extension from the pylorus to the distal duodenum.

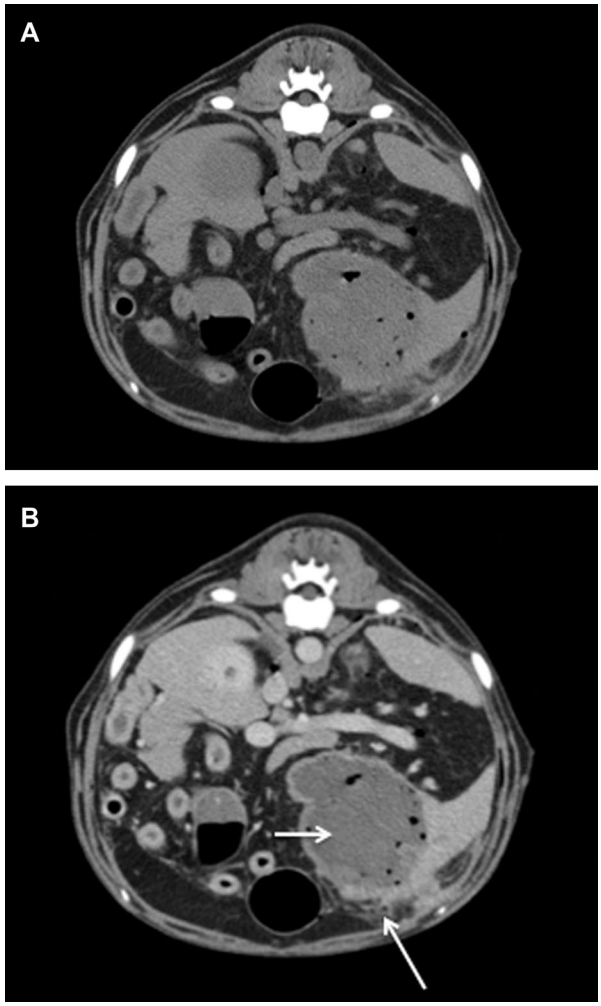

FIG. 1. A 9.5-year-old male neutered mix-breed dog with a splenic abscess secondary to widespread hemangiosarcoma metastasis. Survey transverse plane CT image (A) and transverse plane CT image acquired in the portal venous phase (B) displayed in a soft tissue window. The patient's right is to the reader's left. Note the rim-enhancing mixed gas and fluid-attenuating mass lesion within the splenic tail (short arrow). Multiple gas-attenuating foci are additionally noted within the peritoneal cavity. Mild mesenteric fat stranding is noted along the ventral surface of the mass lesion described (long arrow). Pneumoperitoneum was successfully identified with survey radiography and parenchymal gas with US yielding a surgical diagnosis for all modalities.

In 10/19 (53%) cases, ultrasonographic evaluation of the abdomen was considered only partial due to the inability to visualize specific organs that would normally be included in what is considered a complete ultrasonography examination. These omissions typically consisted of small parts (adrenal glands, sublumbar lymph nodes); although in the case of the traumatic diaphragmatic hernia, ultrasonographic evaluation was limited to a CEUS perfusion study of the herniated spleen alone given that the patient was in respiratory distress. Pneumoperitoneum was not detected sonographically in any of the enrolled cases. Hyperechoic

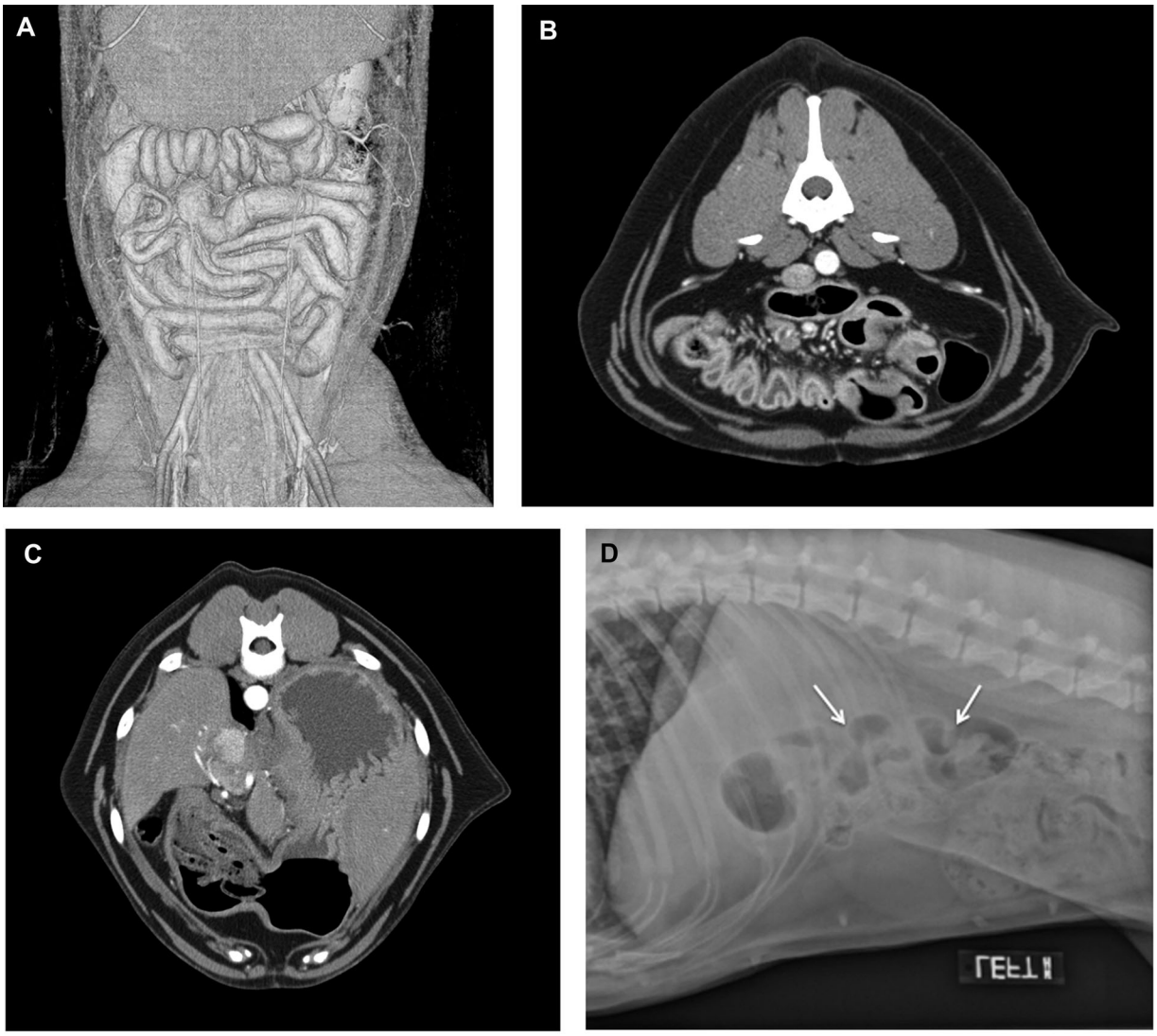

FIG. 2. A 5.1-year-old female spayed mix-breed dog with a linear foreign body where plication was detected using all imaging modalities. The patient's right is to the reader's left (CT) and patient's head to the reader's left (radiograph). CT images are displayed in a soft tissue window. (A) Three-dimensional volume rendering reconstruction acquired in the arterial phase displayed with visible voxel values ranging from 40–203 HU in a dorsal plane. Note the clearly demonstrated marked jejunal plication in the mid abdomen. (B) Transverse plane CT image acquired in the arterial phase at the level of the jejunal plication noted in (A). (C) Transverse plane CT image acquired in the arterial phase at the level of the pylorus where the proximal extension of the linear foreign body is clearly visualized. (D) Left lateral radiographic projection of the abdomen demonstrating marked duodenal plication (white arrows).

mesentery was identified sonographically in 9/19 (47%) cases: splenic abscess formation with rupture, gastric perforation secondary to ulcerative B-cell lymphoma, gastric B-cell lymphoma without perforation, and acute pancreatitis (six cases). Small bowel plication was noted in 4/4 (100%) cases with obstructive small intestinal linear foreign bodies. Gastrointestinal foreign material was considered sonographically visible in 4/6 (66%). A distinct zone of transition was identified in 4/6 (67%) cases with evidence of small intestinal mechanical obstruction. A portion of the small bowel was considered distended in 5/6 (83%) cases. Peritoneal free fluid was detected sonographically in 5/19 (26%) cases. Ultrasonography correctly identified 8/9 (89%) cases as surgical for which a conclusion could be made with imaging findings alone. The false-negative diagnosis was made in the case of gastric perforation due to an inability to identify pneumoperitoneum.

Pending the tentative diagnosis at the time of ultrasonographic evaluation, CEUS was performed in a focused manner on the organ of interest: pancreas (seven cases; acute pancreatitis), stomach wall (two cases; B-cell lymphoma), small intestine (six cases; obstructive foreign bodies), liver (two cases; hepatic abscess formation), spleen (two cases; splenic abscess and transdiaphragmatic splenic herniation). In both cases of gastric B-cell lymphoma, multifocal hypoperfused foci were noted within the gastric

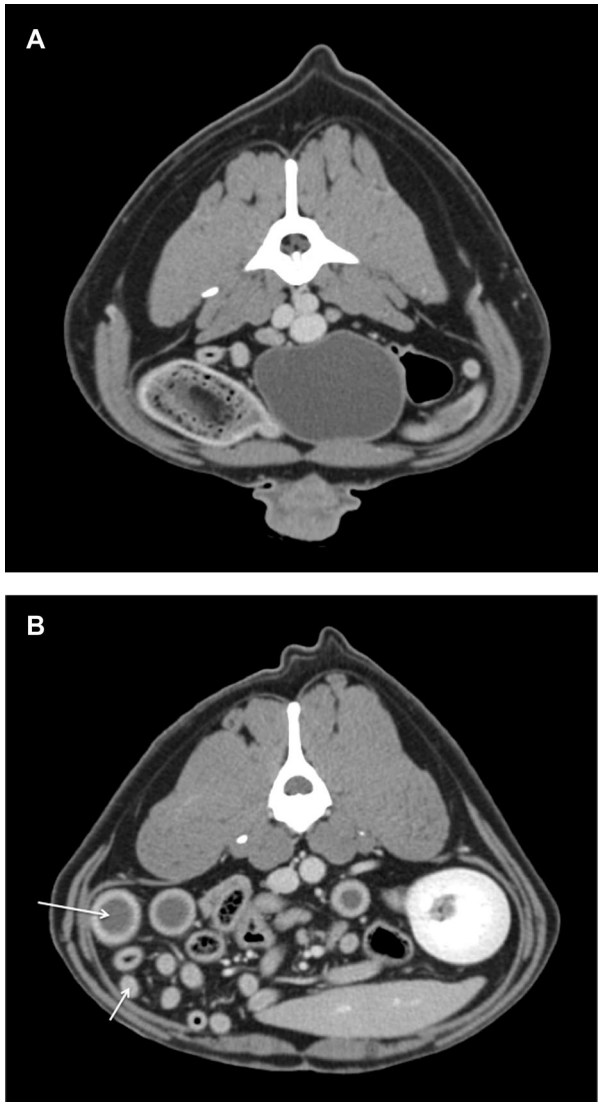

FIG. 3. A 7.1-year-old male intact American Pit Bull Terrier with a corn cob jejunal foreign body. The correct diagnosis of small intestinal mechanical ileus was made with all imaging modalities. Transverse CT image acquired in the portal venous phase and displayed in a soft tissue window. The patient's right is to the reader's left. (A) Note the clearly visible luminal jejunal foreign body with uniform surrounding bowel wall enhancement. The foreign body was removed via enterotomy. (B) Note the two populations of small bowel: empty segment (short arrow), and fluid distended segment (long arrow).

TABLE 1. Agreement Between Modalities for Specific Imaging Findings in 19 Dogs with Acute Abdominal Signs

Imaging finding	κ (Rad vs.US)	κ (Rad vs.CT)	κ (CT vs.US)
Categorical data			
Pneumoperitoneum	0.00	1.00	0.00
Small intestinal plication	0.82	0.82	1.00
Small intestinal distension	0.48	0.50	0.54
Visible GI foreign material	0.56	0.73	0.87
Zone of transition (if small intestinal plication/ distension)	N/A	N/A	0.20
Peritonitis (fat stranding on CT, hyperechoic mesentery on US)	N/A	N/A	0.22
Medical vs.surgical condition	0.78	0.89	0.89
Ordinal data (weighted κ)			
Peritoneal free fluid (CT, US) vs. loss of serosal detail (Rad)	0.60	0.47	0.60

κ = kappa statistic, Rad = Survey Radiography, US = Ultrasound, CT = Computed Tomography, GI = Gastrointestinal, N/A = Not applicable.

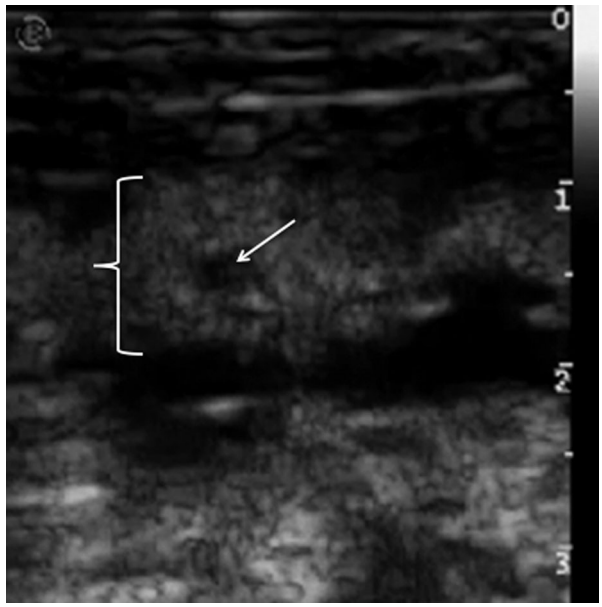

FIG. 4. An 8-year-old female spayed Golden Retriever with a cloth linear foreign body. Contrast-enhanced US image of a segment of affected jejunum with a rounded focal perfusion deficit (white arrow) noted in the near wall (delineated with a white bracket) at peak contrast enhancement. Jejunal resection and anastomosis was performed. Histologically the jejunal mucosa was focally severely ulcerated. The submucosa was severely edematous and the muscle layers contained marked, multifocal hemorrhage.

wall on CEUS. Mural perfusion deficits were noted in 2/6 (33%) cases for which CEUS was performed at the site of a small intestinal foreign body (Fig. 4). Both of these cases required jejunal resection and anastomosis at the time of surgery and both cases underwent spontaneous cardiorespiratory arrest (one during hospitalization and one shortly following discharge). In all seven cases of acute pancreatitis, CEUS successfully identified a hypoperfused parenchymal lesion. When the maximum dimension of a relatively hypoechoic pancreatic lesion on B-mode ultrasonography was compared with the maximal dimension of the same lesion on CEUS (hypoperfused portion only), there was poor agreement with greater disparity at larger lesion dimensions (Fig. 5). In 2/3 (67%) cases for which a hypoperfused or non-enhancing lesion was noted in the pancreas with both CEUS and CE-MDCT respectively, maximum lesion dimension was relatively greater with CE-MDCT (255 vs. 96 mm^2 and 371 vs.184 mm^2). In 2/2 cases for which a hypoperfused or non-enhancing lesion was noted in the liver with both CEUS and and CE-MDCT respectively, maximum lesion dimension was consistently greater with CE-MDCT (1268 vs. 778 mm^2 and 441 vs. 276 mm^2).

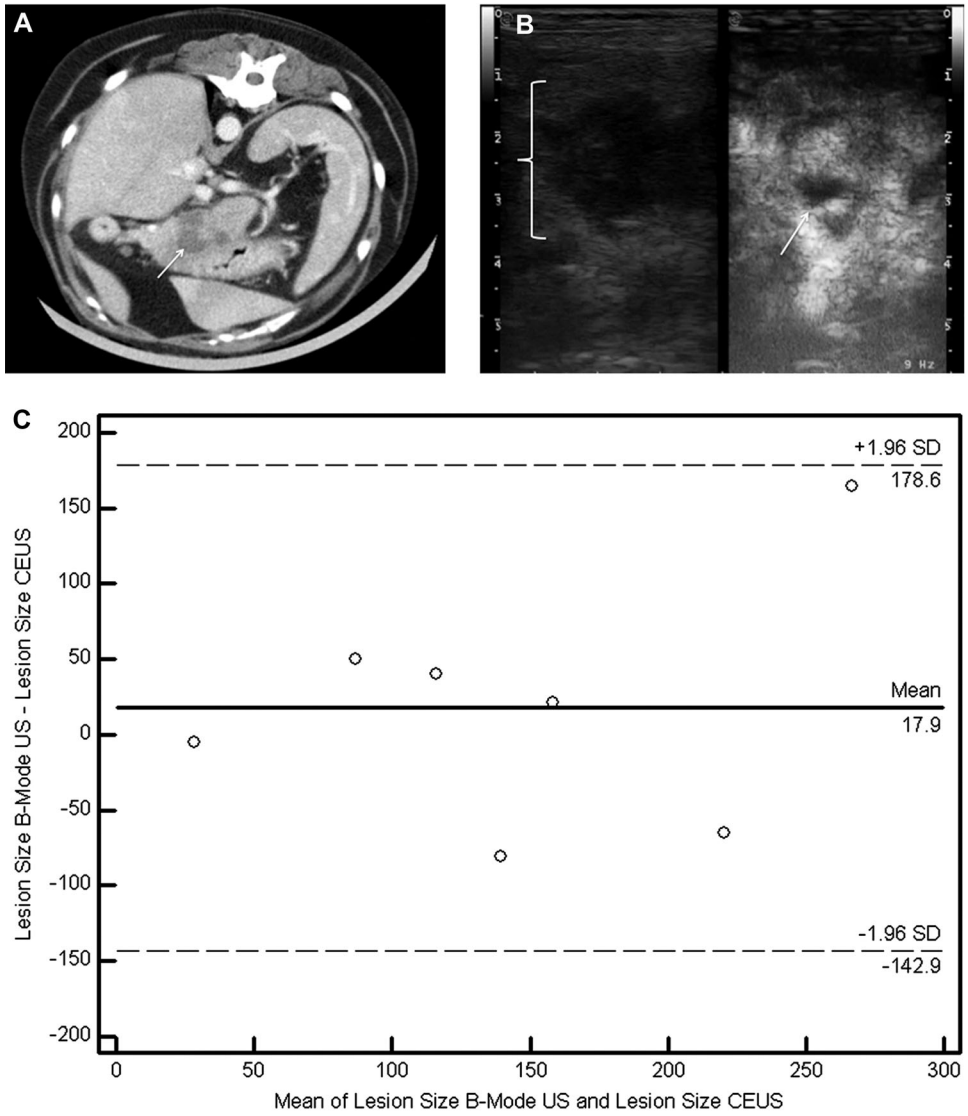

FIG. 5. A 10.8-year-old male intact Shetland Sheepdog with acute pancreatitis. (A) Transverse CT image acquired in the portal venous phase and displayed in a soft tissue window. The patient's right is to the reader's left. Note that there are multiple ill-marginated, relatively non-enhancing, foci within the body of the pancreas (white arrow). (B) B-mode (left) and contrast-enhanced US (CEUS) (right) images of the same region of the pancreas at peak perfusion. Note the poor agreement in the overall size of the hypoechoic lesion noted on B-mode ultrasonography (white bracket) when compared with the relatively small foci of hypoperfusion detected with CEUS (white arrow). (C) Bland–Altman plot. Note poor agreement of pancreatic lesion dimension when measured with B-mode ultrasonography versus CEUS with the greatest discordance identified at larger lesion dimensions. Overall, there is also a tendency for overestimation of lesion size on B-mode ultrasonography when compared with CEUS.

In one case with multifocal non-enhancing hepatic lesions, CE-MDCT detected a greater number of total lesions than CEUS (12 vs. 4, respectively). In 2/3 (67%) cases for which the number of non-enhancing splenic lesions was assessed with both CE-MDCT and CEUS, CE-MDCT detected a greater number of lesions (7 vs. 3 and 5 vs. 1).

When combining data from multiple phases during CT acquisition, all routinely visualized organs could be evaluated with the exception of a single case in which pre-administered barium contrast material within the gastrointestinal tract obscured portions of the cranial abdomen. Computed tomography detected pneumoperitoneum in 2/19 (11%) cases. Overall, the CT imaging feature of mesenteric fat stranding was noted in 6/19 (32%) cases and was associated with a variety of disease processes including splenic abscess formation with rupture secondary to widespread hemangiosarcoma (Fig. 1), gastric perforation secondary to ulcerative B-cell lymphoma (Fig. 6), linear foreign body (two) and acute pancreatitis (two). While there was lack of agreement between the CT feature of fat stranding and the sonographic detection of hyperechoic mesentery, these imaging findings did overlap in four cases

FIG. 6. A 6-year-old male intact Labrador Retriever with a gastric perforation secondary to ulcerative B-cell lymphoma. Pneumoperitoneum was detected with both survey radiography and CT, however, not with US. Transverse CT image acquired in the portal venous phase and displayed in a soft tissue window. The patient's right is to the reader's left. Note the soft tissue attenuating streaky appearance throughout the mesentery in the left craniodorsal abdomen adjacent to the stomach; multiple gas-attenuating foci are noted free within the peritoneal cavity at the same level. Note the nonuniform gastric wall contrast enhancement. Distinct persistently non-enhancing foci were detected within the gatric wall with both CE-MDCT and CEUS. Histologic evaluation of the perigastric adipose tissue described revealed multifocal fat necrosis with infiltration by a large number of leukocytes, admixed with severe edema and fibrin deposition.

including splenic abscess formation secondary to hemangiosarcoma with rupture, gastric B-cell lymphoma with perforation and two cases of acute pancreatitis. Contrast-enhanced MDCT correctly identified small bowel plication in 4/4 (100%) linear foreign body cases. Gastrointestinal foreign material, small bowel distension, and a distinct zone of transition were consistently visualized on CT in all cases of small bowel obstruction (6/6, 100% of cases). Peritoneal free fluid was noted in 3/19 (16%) cases. If a surgical condition could be identified with imaging findings alone, the correct assessment was made with CT in 9/9 (100%) cases.

Contrast-enhanced MDCT identified persistently non-enhancing parenchymal lesions in 3/7 (43%) cases with acute pancreatitis (Fig. 5). In 2/3 (67%) cases for which a non-enhancing pancreatic lesion was noted with both CE-MDCT and CEUS, the maximal dimension of the lesion was greater on CT as described above. Given the small number of cases for which a non-enhancing pancreatic lesion was noted on both modalities, a statistical comparison of relative lesion size could not be performed. In both cases for which multifocal non-enhancing foci were noted within the gastric wall on CEUS, the same findings were reported on CE-MDCT. In 2/6 (33%) cases for which CEUS was performed at the site of a small intestinal foreign body, mural perfusion deficits were noted for which CE-MDCT failed to detect any deficits in contrast enhancement (Fig. 4). When comparing the maximal dimension and total number of non-enhancing hypoperfused hepatic lesions on CE-MDCT vs. CEUS respectively, CT consistently achieved a larger maximal dimension and showed a trend toward a relatively higher total number of lesions as described above. As a comparison of liver lesion size and number was performed on only two cases, this data could not be accurately assessed statistically. Contrast-enhanced MDCT and CEUS evaluation of discrete splenic lesions revealed similar results showing a greater number of lesions on CT as described above. Again, due to the small number of cases for which a comparison was possible, statistical analysis could not be performed.

TABLE 2. Frequencies of Select Imaging Findings for Three Modalities in 19 Dogs with Acute Abdominal Signs

Imaging finding	RAD	US	CT
Pneumoperitoneum	2/19 (11%)	0/19 (0%)	2/19 (11%)
Small intestinal plication	3/4 (75%)	4/4 (100%)	4/4 (100%)
Small intestinal distension	4/6 (67%)	5/6 (83%)	6/6 (100%)
Visible GI foreign material	5/6 (83%)	4/6 (67%)	6/6 (100%)
Zone of transition (if small intestinal plication/ distension)	N/A	4/6 (67%)	6/6 (100%)
Peritonitis (hyperechoic mesentery on US, fat stranding on CT)	N/A	9/19 (47%)	6/19 (32%)
Peritoneal free fluid (US, CT)	N/A	5/19 (26%)	3/19 (16%)
Surgical condition	8/9 (89%)	8/9 (89%)	9/9 (100%)

Rad = Survey Radiography, US = B-Mode Ultrasound, CT = Computed Tomography, GI = Gastrointestinal, N/A = Not applicable.

Overall, the majority of imaging features showed at least moderate agreement ($\kappa > 0.41$) between modalities (Table 1). Sensitivity, specificity, PPV, NPV, and accuracy of each modality for the diagnosis of a surgical condition (excluding the two cases for which cytology was an absolute requirement) were as follows: CE-MDCT (100% in all cases), ultrasonography and survey radiography (sensitivity 89%, specificity 100%, PPV 100%, NPV 89%, and accuracy 94%). Select imaging findings across survey imaging modalities are further summarized in Table 2.

Discussion

Targeted helical CT of the abdomen is the current standard modality for evaluation of the human acute abdominal patient.[70–72] In a recent retrospective study, 72% of human patients whose abdominal radiography results were considered normal were found to have abnormal findings at follow-up imaging, including major abnormalities in 78% of cases.[73] A multicenter prospective trial evaluating human patients presenting to the emergency department with abdominal pain revealed similar limitations. A total of 1021 patients were included in the study. The diagnosis

following radiographic evaluation was correct in only 50% of patients. The authors concluded therefore, that plain radiography in human patients with acute abdominal pain was of limited value.[74]

Conversely, survey radiography and routine B-mode US are the current standard modalities for evaluating veterinary clinical patients with acute abdominal signs. This is primarily due to the higher expense of CT and frequent need for general anesthesia for CT scans in the majority of veterinary practices. Recently, awake and minimally sedated CE-MDCT protocols using 16-slice technology have been used both safely and successfully in the evaluation of canine and feline patients with acute abdominal and respiratory conditions respectively.[58,75] Survey radiography and routine ultrasonography have multiple limitations that may be overcome by the CE-MDCT protocol used in our study population. These limitations include, but are not limited to, the following: possibility of prolonged image acquisition and patient discomfort (with respect to abdominal ultrasonography), superimposition/interference of organs of interest, inability/difficulty visualizing small parts, nonspecific imaging findings (radiography), and poor sensitivity for critical surgical lesions such as pneumoperitoneum (ultrasonography). In our study, a large number of ultrasonography exams (53%) were considered only partial due to one or more of the reasons listed above. As a result, these modalities are often performed sequentially to maximize diagnostic potential. A distinct advantage of ultrasonography, however, is the routine identification of small volumes of peritoneal free fluid, which if aspirated and confirmed cytologically in the case of a septic abdomen of unknown etiology, is critical in pursuing prompt surgical intervention.

Contrast-enhanced MDCT and survey radiography detected pneumoperitoneum in two cases for which ultrasonography findings were negative, accounting for poor statistical agreement for this specific imaging feature. Gastric perforation secondary to B-cell lymphoma and splenic abscess (due to widespread hemangiosarcoma) were confirmed histologically in these two cases. In the case of gastric perforation, identification of pneumoperitoneum was essential in establishing a surgical diagnosis, therefore, accounting for the single false-negative result in the case of ultrasonography. This single false-negative resulted in the minimally decreased sensitivity, NPV, and ultimately accuracy of ultrasonography relative to CT for differentiating surgical from non-surgical disease with imaging findings alone. The case of splenic abscess formation with rupture was correctly classified as surgical with ultrasonography findings alone due to the presence of gas-containing parenchymal cavitary lesions (Fig. 1). CT and survey radiography are expected to have an increased sensitivity over ultrasonography in the detection of pneumoperitoneum, however, the limited number of positive cases in our study can only suggest an impression rather than a proven statistical advantage.

The CT feature of fat stranding, defined as an abnormal increased attenuation in fat (mesenteric fat in the context of this study), is characterized by a proposed underlying pathophysiologic process of increased edema and engorgement of local lymphatics.[59] This CT finding may manifest with multiple patterns including a subtle hazy/ground-glass like appearance in the presence of mild inflammation or a more reticular pattern with more well-defined linear areas of increased attenuation with more severe inflammatory conditions. A reticulonodular pattern may also be observed in association with neoplastic disease.[59] Not unexpectedly, this CT feature is identified across a broad spectrum of disease processes including, but not limited to, disease originating from the bowel, pancreas, gallbladder, and upper urinary tract.[59] This lack of specificity is consistent with our study findings for which fat stranding was noted across a variety of pathological processes including a case of solid organ abscess formation, small bowel obstructive disease, primary gastric neoplasia with perforation and acute pancreatitis. While the extent of fat stranding was not specifically quantified, this was subjectively most severe in the case of gastric perforation secondary to B-cell lymphoma. The affected mesentery was evaluated histologically in this case revealing multifocal fat necrosis with infiltration by a large number of leukocytes, admixed with severe edema and fibrin deposition (Fig. 6). While there was only fair statistical agreement between the CT feature of fat stranding and the sonographic detection of hyperechoic mesentery, these imaging findings did overlap in four cases including splenic abscess formation secondary to hemangiosarcoma with rupture (Fig. 1), gastric B-cell lymphoma with perforation and two cases of acute pancreatitis. The lack of a statistical agreement between modalities is likely due to a combination of the small number of cases evaluated and frequently limited field of view in the case of abdominal ultrasonography. We propose that the CT identification of focal fat stranding or the sonographic detection of hyperechoic mesentery, should prompt the radiologist to perform a more rigorous evaluation of the regional viscera as these imaging features were frequently identified adjacent to clinically significant lesions. While this technique is helpful in identifying an organ of interest, differential diagnoses remain numerous. Future studies that aim to specifically quantify the degree of fat stranding may be beneficial as disproportionate fat stranding in human patients with acute abdominal pain may help narrow the differential diagnosis of GI disorders, for example.[62]

In the characterization of small intestinal mechanical obstruction secondary to foreign material, plication associated with a linear foreign body was correctly identified in all four cases with CE-MDCT and ultrasonography. Survey radiography failed to detect small bowel plication in a linear

foreign body that extended from the pyloric antrum to the distal duodenum resulting in a false-negative diagnosis of a surgical abdomen and therefore minimally reduced sensitivity, NPV, and overall accuracy relative to CE-MDCT for the differentiation of surgical vs. medical underlying disease. Small intestinal foreign material, small bowel distension, and a distinct zone of transition were consistently visualized on CT. Small intestinal foreign material and luminal distension were noted in the majority of cases with survey radiography and ultrasonography. Zone of transition was not specifically assessed radiographically due to visceral superimposition, however, was identified in 4/6 (67%) cases sonographically.

Overall, peritoneal free fluid was identified most frequently with abdominal ultrasonography (5/19, 26%). Statistical agreement was moderate for the sonographic or CT identification of peritoneal free fluid and loss of peritoneal serosal detail on survey radiographs. While there is not a perfect reference standard for the confirmation of the presence and degree of peritoneal effusion, our impression is that ultrasonography may be more sensitive in the detection of small volumes of peritoneal fluid when compared with CE-MDCT.

Focused CEUS proved beneficial in the identification of multiple small bowel and pancreatic perfusion deficits that were not clearly identified with CE-MDCT. This can be explained by the improved spatial and temporal resolution of ultrasonography relative to CT and the exquisite sensitivity of microbubble contrast material for assessment of perfusion deficiencies. In two such cases with small intestinal foreign bodies, jejunal resection and anastomosis was required and patient outcome was ultimately poor. The clinical relevance of the small bowel perfusion deficits detected exclusively with CEUS remains unclear. In our study, the surgical approach (specifically bowel resection) was selected without knowledge of the CT or CEUS perfusion findings. Further studies investigating the size and number of bowel perfusion deficits across multiple modalities as it relates to intra-operative findings, histology and patient outcome are needed for further clarification. Similarly, in the case of acute pancreatitis, multiple perfusion deficits were identified exclusively with CEUS. Patient prognosis was, however, excellent in the majority of cases. It is possible that our patient population represents a milder form of the disease given the relatively small overall size of identified hypoperfused lesions. Small lesion size could potentially account for the inability to consistently identify non- or poorly enhancing parenchymal lesions with CE-MDCT. A prospective study evaluating the estimated percentage of poorly enhancing pancreatic tissue as it relates to long-term outcome and need for intervention is necessary to clarify these preliminary imaging findings. Furthermore, pancreatic lesion size assessment with B-mode ultrasonography showed poor agreement with associated CEUS findings suggesting that CEUS may provide more accurate information when assessing the actual size of a suspect hypoperfused or necrotic lesion with ultrasonography. Overall, there was a tendency for CEUS to underestimate the total number and maximum surface area of parenchymal lesions that were evaluated with both CEUS and CE-MDCT. This is not surprising given the limited field of view of ultrasonography relative to CT. Prolonged CEUS evaluation with a directed attempt to image the entire liver and spleen, for example, may have resulted in more consistent results. This is not, however, practical in the clinical setting especially if prolonged scan duration does not ultimately result in a change in intervention.

Given the exquisite sensitivity of CEUS in the characterization of visceral perfusion, CEUS has recently emerged in human medicine as a modality of interest in the evaluation of acute abdominal conditions including ischemic bowel disease[76,77] and acute pancreatitis.[78,79] The veterinary literature thus far remains predominantly limited to characterization of normal visceral perfusion[80–87] and clinical conditions that are not typically associated with acute abdominal signs including lymphomatous lymph nodes, portosystemic shunt, and focal hepatic, splenic, or renal lesions.[88–97] Given the data reported in our study, however, CEUS will likely provide similar promise as a method of enhancing the diagnostic potential of conventional B-mode ultrasonography in veterinary clinical patients with acute abdominal signs.

In the context of our patient population, when a surgical condition could be diagnosed with imaging findings alone, CT was successful in 100% of cases. No false-positive diagnoses, however, were made with any of the modalities evaluated yielding a PPV of 100% in all cases. Sensitivity, NPV, and accuracy for the diagnosis of a surgical condition were only minimally decreased in survey radiography and ultrasonography when compared with MDCT for the reasons stated above. Overall, data suggests that CT shows only slight improvement in accuracy when differentiating surgical from non-surgical conditions, however, data may be skewed by a relative bias toward the diagnostic accuracy of ultrasonography given that the majority of cases required the sonographic detection of a specified lesion for study inclusion.

Although the benefit of arterial-phase imaging in CT was not specifically assessed in this study due to our small sample size and heterogeneity of underlying disease processes, arterial-phase imaging warrants further investigation given the critical implications on overall prognosis in the human patient with acute abdominal pain. In a case series describing the contrast-enhanced CT diagnosis of acute bowel infarction in people, the following findings reportedly demonstrate a specificity of greater than 95%: superior mesenteric artery or vein thrombosis, intramural bowel gas, portal vein gas, focal lack of bowel enhancement, and ischemia of other

FIG. 7. A 7-year-old female spayed Scottish Terrier with gastric B-cell lymphoma. Dorsal plane maximum intensity projection reconstruction with 43.5-mm slab thickness, window width of 385, and window level of 152 acquired in the arterial phase. The patient's right is to the reader's left. Note the large number of anomalous tortuous arterial vessels supplying the gastric wall.

organs.[98] In a separate study, arterial obstruction resulted in an 89% mortality rate while venous obstruction only resulted in 11%.[99] It is possible that arterial-phase imaging may also provide indications of underlying malignancy as we observed both increased vessel number and tortuosity in an enrolled case of gastric B-cell lymphoma (Fig. 7). This is not unexpected given similar CEUS imaging features in malignant focal splenic and renal lesions in small animal clinical patients.[93,97]

Primary limitations of our study include small overall sample size and concurrent heterogeneity of specific underlying disease processes. Our primary goal, however, was not in the characterization of specific diseases but rather the assessment of agreement between multiple imaging modalities for specific imaging findings and in the ability to differentiate surgical from non-surgical conditions. Given the rigorous inclusion criteria, an additional limitation of this study is the relatively narrow spectrum in severity of acute abdominal disease as milder forms of acute abdominal pain (namely self-limiting gastroenteritis) were not included. This may have resulted in overestimation of diagnostic accuracy for all modalities evaluated as it relates to the differentiation of surgical vs. medical conditions. As the majority of cases required sonographic detection of a specified lesion for study inclusion, a relative bias contributing to the overall accuracy of ultrasonography in differentiating surgical from medical conditions must be considered. Further studies evaluating a spectrum of specific disease entities (e.g. small intestinal obstruction due to foreign body, gastrointestinal, or visceral neoplasms, acute pancreatitis) are necessary in an attempt to determine if a correlation exists between the identification of specific lesions and patient outcome/prognosis.

We propose that CE-MDCT may be used safely and effectively as a preliminary imaging screening modality for canine patients with acute abdominal signs as this will provide both a rapid and accurate diagnosis with minimal patient discomfort. Overall accuracy for all modalities evaluated, was however, excellent. If evaluated concurrently, survey radiography and ultrasonography would have yielded an accuracy of 100% for the differentiation of surgical from non-surgical conditions. Furthermore, given the improved sensitivity in the evaluation of bowel and pancreatic perfusion relative to CT, focused CEUS of lesions identified on preliminary CE-MDCT or B-mode ultrasonography may provide great promise in the diagnostic assessment of critically ill canine patients.

REFERENCES

1. Lamb CR, Simpson KW. Ultrasonographic findings in cholecystokinin induced pancreatitis in dogs. Vet Radiol Ultrasound 1995;36:139–145.
2. Nyland TG, Mulvany MH, Strombeck DR. Ultrasonic features of experimentally induced, acute pancreatitis in the dog. Vet Radiol 1983;24:260–266.
3. Hecht S, Henry G. Sonographic evaluation of the normal and abnormal pancreas. Clin Tech Small Anim Pract 2007;22:115–121.
4. Murtaugh RJ, Herring DS, Jacobs RM, DeHoff WD. Pancreatic ultrasonography in dogs with experimentally induced acute pancreatitis. Vet Radiol 1985;26:27–32.
5. Saunders HM. Ultrasonography of the pancreas. Probl Vet Med 1991;3:583–603.
6. Hess RS, Saunders HM, Van Winkle TJ, et al. Clinical, clinicopathologic, radiographic, and ultrasonographic abnormalities in dogs with fatal acute pancreatitis: 70 cases (1986–1995). JAVMA 1998;213:665–670.
7. Jaeger JQ, Mattoon JS, Bateman SW, Morandi F. Combined use of ultrasonography and contrast enhanced computed tomography to evaluate acute necrotizing pancreatitis in two dogs. Vet Radiol Ultrasound 2003;44:72–79.
8. Hoffman KL. Sonographic signs of gastroduodenal linear foreign body in 3 dogs. Vet Radiol Ultrasound 2003;44:466–469.
9. Kaser-Hotz B, Hauser B, Arnold P. Ultrasonographic findings in canine gastric neoplasia in 13 patients. Vet Radiol Ultrasound 1996;37:51–56.
10. Lamb CR, Grierson J. Ultrasonographic appearance of primary gastric neoplasia in 21 dogs. J Small Anim Pract 1999;40:211–215.
11. Penninck DG, Matz M, Tidwell A. Ultrasonography of gastric ulceration in the dog. Vet Radiol Ultrasound 1997;38:308–312.
12. Penninck DG, Moore AS, Gliatto J. Ultrasonography of canine gastric epithelial neoplasia. Vet Radiol Ultrasound 1998;39:342–348.
13. Penninck DG, Mitchell SL. Ultrasonographic detection of ingested and perforating wooden foreign bodies in four dogs. JAVMA 2003;223:206–209.
14. Penninck DG, Nyland TG, Kerr LY, Fisher PE. Ultrasonographic evaluation of gastrointestinal diseases in small animals. Vet Radiol 1990;31:134–141.
15. Rivers BJ, Walter PA, Johnston GR, et al. Canine gastric neoplasia: utility of ultrasonography in diagnosis. J Am Anim Hosp Assoc 1997;33:144–155.

16. Tidwell AS, Penninck DG. Ultrasonography of gastrointestinal foreign bodies. Vet Radiol Ultrasound 1992;33:160–169.

17. Boysen SR, Tidwell AS, Penninck DG. Ultrasonographic findings in dogs and cats with gastrointestinal perforation. Vet Radiol Ultrasound 2003;44:556–564.

18. Ferrell EA, Graham JP. Ultrasound corner diagnosis of pneumoperitoneum. Vet Radiol Ultrasound 2003;44:307–308.

19. Sharma A, Thompson MS, Scrivani PV, et al. Comparison of radiography and ultrasonography for diagnosing small-intestinal mechanical obstruction in vomiting dogs. Vet Radiol Ultrasound 2011;52:248–255.

20. Tyrrell D, Beck C. Survey of the use of radiography vs. ultrasonography in the investigation of gastrointestinal foreign bodies in small animals. Vet Radiol Ultrasound 2006;47:404–408.

21. Grassi R, Romano S, Pinto A, Romano L. Gastro-duodenal perforations: conventional plain film, ultrasonography and CT findings in 166 consecutive patients. Eur J Radiol 2004;50:30–36.

22. Grassi R, Romano S, D'Amario F, et al. The relevance of free fluid between intestinal loops detected by sonography in the clinical assessment of small bowel obstruction in adults. Eur J Radiol 2004;50:5–14.

23. Chiu YH, Chen JD, Tiu CM, et al. Reappraisal of radiographic signs of pneumoperitoneum at emergency department. Am J Emerg Med 2009;27:320–327.

24. Barthez PY, Begon D, Delisle F. Effect of contrast medium dose and image acquisition timing on ureteral opacification in the normal dog as assessed by computed tomography. Vet Radiol Ultrasound 1998;39:524–527.

25. Lee S, Jung J, Chang J, et al. Evaluation of triphasic helical computed tomography of the kidneys in clinically normal dogs. J Vet Res 2011;72:345–349.

26. Moe L, Lium B. Computed tomography of hereditary multifocal renal cystadenocarcinomas in german shepherd dogs. Vet Radiol Ultrasound 1997;38:335–343.

27. Samii VF. Inverted contrast medium-urine layering in the canine urinary bladder on computed tomography. Vet Radiol Ultrasound 2005;46:502–505.

28. Samii VF, Mcloughlin MA, Mattoon JS, et al. Digital fluoroscopic excretory urography, digital fluoroscopic urethrography, helical computed tomography, and cystoscopy in 24 dogs with suspected ureteral ectopia. J Vet Intern Med 2004;18:271–281.

29. Secrest S, Britt L, Cook C. Imaging diagnosis-bilateral orthotopic ureteroceles in a dog. Vet Radiol Ultrasound 2011;52:448–450.

30. Yamazoe K, Ohashi F, Kadosawa T, et al. Computed tomography on renal masses in dogs and cats. J Vet Med Sci. 1994;56:813–816.

31. Patsikas MN, Rallis T, Kladakis S, Dessiris AK. Computed tomography diagnosis of isolated splenic torsion in a dog. Vet Radiol Ultrasound 2001;42:235–237.

32. Ohta H, Takagi S, Murakami M, et al. Primary splenic torsion in a boston terrier. J Vet Med Sci 2009;71:1533–1535.

33. Fife WD, Samii VF, Drost WT, et al. Comparison between malignant and nonmalignant splenic masses in dogs using contrast-enhanced computed tomography. Vet Radiol Ultrasound 2004;45:289–297.

34. Frank P, Mahaffey M, Egger C, Cornell KK. Helical computed tomographic portography in ten normal dogs and ten dogs with a portosystemic shunt. Vet Radiol Ultrasound 2003;44:392–400.

35. Zwingenberger AL, Schwarz T. Dual-phase CT angiography of the normal canine portal and hepatic vasculature. Vet Radiol Ultrasound 2004;45:117–124.

36. Winter MD, Kinney LM, Kleine LJ. Three-dimensional helical computed tomographic angiography of the liver in five dogs. Vet Radiol Ultrasound 2005;46:494–499.

37. Zwingenberger AL, McLear RC, Weisse C. Diagnosis of arterioportal fistulae in four dogs using computed tomographic angiography. Vet Radiol Ultrasound. 2005;46:472–477.

38. Zwingenberger AL, Schwarz T, Saunders HM. Helical computed tomographic angiography of canine portosystemic shunts. Vet Radiol Ultrasound 2005;46:27–32.

39. Bertolini G, Rolla EC, Zotti A, Caldin M. Three-dimensional multislice helical computed tomography techniques for canine extra-hepatic portosystemic shunt assessment. Vet Radiol Ultrasound 2006;47:439–443.

40. Echandi RL, Morandi F, Daniel WT, et al. Comparison of transplenic multidetector CT portography to multidetector CT-angiography in normal dogs. Vet Radiol Ultrasound 2007;48:38–44.

41. Stieger SM, Zwingenberger A, Pollard RE, et al. Hepatic volume estimation using quantitative computed tomography in dogs with portosystemic shunts. Vet Radiol Ultrasound 2007;48:409–413.

42. Zwingenberger AL, Shofer FS. Dynamic computed tomographic quantitation of hepatic perfusion in dogs with and without portal vascular anomalies. Am J Vet Res 2007;68:970–974.

43. Irausquin RA, Scavelli TD, Corti L, et al. Comparative evaluation of the liver in dogs with a splenic mass by using ultrasonography and contrast-enhanced computed tomography. Can Vet J 2008;49:46–52.

44. Kummeling A, Vrakkin DJE, Roghuizen J, et al. Hepatic volume measurements in dogs with extrahepatic congenital portosystemic shunts before and after surgical attenuation. J Vet Intern Med 2010;24:114–119.

45. Nelson NC, Nelson LL. Anatomy of extrahepatic portosystemic shunts in dogs as determined by computed tomography angiography. Vet Radiol Ultrasound 2011;52:498–506.

46. Zwingenberger AL, Spriet M, Hunt GB. Imaging diagnosis-portal vein aplasia and interruption of the caudal vena cava in three dogs. Vet Radiol Ultrasound 2011;52:444–447.

47. Robben JH, Pollak YWEA, Kirpensteijn J, et al. Comparison of ultrasonography, computed tomography, and single-photon emission computed tomography for the detection and localization of canine insulinoma. J Vet Intern Med 2005;19:15–22.

48. Cáceres AV, Zwingenberger AL, Hardam E, et al. Helical computed tomographic angiography of the normal canine pancreas. Vet Radiol Ultrasound 2006;47:270–278.

49. Yasuda D, Fujita M, Yasuda S, et al. Usefulness of MRI compared with CT for diagnosis of mesenteric lymphoma in a dog. J Vet Med Sci 2004;66:1447–1451.

50. Spector DI, Fischetti AJ, Kovak-McClaran JR. Computed tomographic characteristics of intrapelvic masses in dogs. Vet Radiol Ultrasound 2011;52:71–74.

51. Bertolini G, Furlanello T, De Lorenzi D, Caldin M. Computed tomographic quantification of canine adrenal gland volume and attenuation. Vet Radiol Ultrasound 2006;47:444–448.

52. Bertolini G, Furlanello T, Drigo M, Caldin M. Computed tomographic adrenal gland quantification in canine adrenocorticotroph hormone-dependent hyperadrenocorticism. Vet Radiol Ultrasound 2008;49:449–453.

53. Schultz RM, Wisner ER, Johnson EG, Macleod JS. Contrast-enhanced computed tomography as a preoperative indicator of vascular invasion from adrenal masses in dogs. Vet Radiol Ultrasound 2009;50:625–629.

54. Terragni R, Vignoli M, Rossi F, et al. Stomach wall evaluation using helical hydro-computed tomography. Vet Radiol Ultrasound 2012;53:402–405.

55. Yamada K, Morimoto M, Kishimoto M, Wisner ER. Virtual endoscopy of dogs using multi-detector row CT. Vet Radiol Ultrasound 2007;48:318–322.

56. Fields EL, Robertson ID, Brown JC. Optimization of contrast-enhanced multidetector abdominal computed tomography in sedated canine patients. Vet Radiol Ultrasound 2012;53:507–512.

57. Fields EL, Robertson ID, Osborne JA, Brown JC. Comparison of abdominal computed tomography and abdominal ultrasound in sedated dogs. Vet Radiol Ultrasound 2012;53:513–517.

58. Shanaman MM, Hartman SK, O'Brien RT. Feasibility for using dual-phase contrast-enhanced multi-detector helical computed tomography to evaluate awake and sedated dogs with acute abdominal signs. Vet Radiol Ultrasound 2012; 53:605–612.

59. Thornton E, Mendiratta-Lala M, Siewert B, Eisenberg RL. Patterns of fat stranding. AJR 2011;197:W1–W14.

60. Wiesner W, Hauser A, Steinbrich W. Accuracy of multidetector row computed tomography for the diagnosis of acute bowel ischemia in a non-selected study population. Eur Radiol 2004;14:2347–2356.

61. Sahani DV, Sainani NI, Deshpande V, et al. Autoimmune pancreatitis: disease evolution, staging, response assessment, and CT features that predict response to corticosteroid therapy. Radiology 2008;250:118–129.

62. Pereira JM, Sirlin CB, Pinto PS, et al. Disproportionate fat stranding-a helpful CT sign in patients with acute abdominal pain. Radiographics 2004;24:703–715.

63. Horton KM, Fishman EK. CT angiography of the mesenteric circulation. Radiol Clin North Am 2010;48:331–345.

64. Hainaux B, Agneessens E, Bertinotti R, et al. Accuracy of MDCT in predicting site of gastrointestinal tract perforation. Am J Roentgenol 2006;187:1179–1183.

65. Nyland TG, Mattoon JS. Small animal diagnostic ultrasound second edition. Saunders, Philadelphia, PA. 2002.

66. Graham JP, Lord PF, Harrison JM. Quantitative estimation of intestinal dilation as a predictor of obstruction in the dog. J Small Anim Pract 1998;39:521–524.

67. Shapiro SS, Wilk MB. An analysis of variance test for normality (complete samples). Biometrika 1965;52:591–611.

68. Levene H. Robust tests for equality of variances. Ingram Olkin, Harold Hotelling, et alia. Stanford University Press. 1960:278–292.

69. Jakobssen U, Westergren A. Statistical methods for assessing agreement for ordinal data. Scand J Caring Sci 2005;19:427–431.

70. Urban BA, Fishman EK. Tailored helical CT evaluation of acute abdomen. Radiographics 2000;20:725–749.

71. Urban BA, Fishman EK. Targeted helical CT of the acute abdomen: appendicitis, diverticulitis, and small bowel obstruction. Semin Ultrasound CT MRI 2000;21:20–39.

72. Gore RM, Miller FH, Pereles FS, et al. Helical CT in the evaluation of the acute abdomen. AJR 2000;174:901–913.

73. Kellow ZS, MacInnes M, Kurzencwyg D, et al. The role of abdominal radiography in the evaluation of the nontrauma emergency patient. Radiology. 2008;248:887–893.

74. van Randen A, Laméris W, Luitse JSK, et al. The role of plain radiographs in patients with acute abdominal pain at the ED. Am J Emerg Med 2011;29:582–589.

75. Oliveira CR, Mitchell MA, O'Brien RT. Thoracic computed tomography in feline patients without use of chemical restraint. Vet Radiol Ultrasound 2011;52:368–376.

76. Hamada T, Yamauchi M, Tanaka M, et al. Prospective evaluation of contrast-enhanced ultrasonography with advanced dynamic flow for the diagnosis of intestinal ischaemia. Br J Radiol 2007;80:603–608.

77. Hata J, Kamada T, Haruma K, Kusunoki H. Evaluation of bowel ischemia with contrast-enhanced US: initial experience. Radiology 2005;236:712–715.

78. Golea A, Badea R, Socaciu M, et al. Quantitative analysis of tissue perfusion using contrast-enhanced transabdominal ultrasound (CEUS) in the evaluation of the severity of acute pancreatitis. Med Ultrason 2010;12:198–204.

79. Ripollés T, Martínez MJ, López E, et al. Contrast-enhanced ultrasound in the staging of acute pancreatitis. Eur Radiol 2010;20:2518–2523.

80. Bahr A, Wrigley R, Salman M. Quantitative evaluation of imagent as an ultrasound contrast medium in dogs. Vet Radiol Ultrasound 2000;41: 50–55.

81. Bigliardi E, Ferrari L. Contrast-enhanced ultrasound of the normal canine prostate gland. Vet Radiol Ultrasound 2010;52:107–110.

82. Gaschen L, Angelette NIK, Stout R. Contrast-enhanced harmonic ultrasonography of medial iliac lymph nodes in healthy dogs. Vet Radiol Ultrasound 2010;51:634–637.

83. Jiménez DA, O'Brien RT, Wallace JD, Klocke E. Intraoperative contrast-enhanced ultrasonography of normal canine jejunum. Vet Radiol Ultrasound. 2011;52:196–200.

84. Johnson-Neitman JL, O'Brien RT, Wallace JD. Quantitative perfusion analysis of the pancreas and duodenum in healthy dogs by use of contrast-enhanced ultrasonography. Am J Vet Res 2012;73:385–92.

85. Nyman HT, Kristensen AT, Kjelgaard-Hansen M, McEvoy FJ. Contrast-enhanced ultrasonography in normal canine liver. Evaluation of imaging and safety parameters. Vet Radiol Ultrasound 2005;46:243–250.

86. Pey P, Vignoli M, Haers H, et al. Contrast-enhanced ultrasonography of the normal canine adrenal gland. Vet Radiol Ultrasound 2011;52:560–567.

87. Waller KR, O'Brien RT, Zagzebski JA. Quantitative contrast ultrasound analysis of renal perfusion in normal dogs. Vet Radiol Ultrasound 2007;48:373–377.

88. Ivančić M, Long F, Seiler GS. Contrast harmonic ultrasonography of splenic masses and associated liver nodules in dogs. J Am Vet Med Assoc 2009;234:88–94.

89. Kanemoto H, Ohno K, Nakashima K, et al. Characterization of canine focal liver lesions with contrast-enhanced ultrasound using a novel contrast agent—sonazoid. Vet Radiol Ultrasound 2009;50:188–194.

90. Nakamura K, Sasaki N, Murakami M, et al. Contrast-enhanced ultrasonography for characterization of focal splenic lesions in dogs. J Vet Intern Med 2010;24:1290–1297.

91. O'Brien RT, Iani M, Matheson J, et al. Contrast harmonic ultrasound of spontaneous liver nodules in 32 dogs. Vet Radiol Ultrasound 2004;45:547–553.

92. Ohlerth S, Dennler M, Rüefli E, et al. Contrast harmonic imaging characterization of canine splenic lesions. J Vet Intern Med 2008;22:1095–1102.

93. Rossi F, Leone VF, Vignoli M, et al. Use of contrast-enhanced ultrasound for characterization of focal splenic lesions. Vet Radiol Ultrasound 2008;49:154–164.

94. O'Brien RT. Improved detection of metastatic hepatic hemangiosarcoma nodules with contrast ultrasound in three dogs. Vet Radiol Ultrasound 2007;48:146–148.

95. Salwei RM, O'Brien RT, Matheson JS. Use of contrast harmonic ultrasound for the diagnosis of congenital portosystemic shunts in three dogs. Vet Radiol Ultrasound 2003;44:301–305.

96. Salwei RM, O'Brien RT, Matheson JS. Characterization of lymphomatous lymph nodes in dogs using contrast harmonic and power Doppler ultrasound. Vet Radiol Ultrasound 2005;46:411–416.

97. Haers H, Vignoli M, Paes G, et al. Contrast harmonic ultrasonographic appearance of focal space-occupying renal lesions. Vet Radiol Ultrasound 2010;51:516–522.

98. Gellett LR, Harries SR, Roobottom CA. Urgent contrast enhanced computed tomography in the diagnosis of acute bowel infarction. Emerg Med J 2002;19:480–481.

99. Moschetta M, Stabile Ianora AA, Pedote P, et al. Prognostic value of multidetector computed tomography in bowel infarction. Radiol Med 2009;114:780–791.